

AD-A183 233

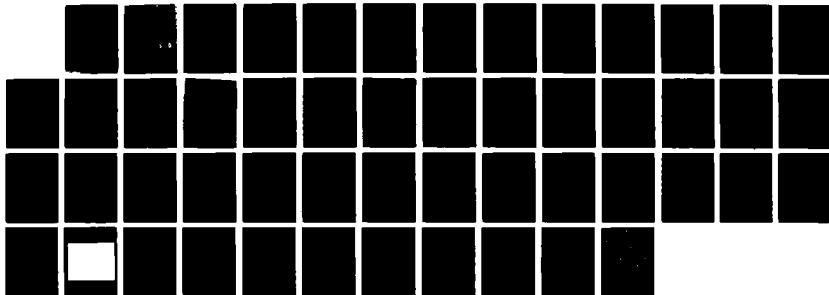
ELECTRO-OPTICAL CHARACTERIZATION OF THE TEKTRONIX  
TK312M-011 CCD (CHARGE-... (U) ARIZONA UNIV TUCSON DEPT  
OF CHEMISTRY P M EPPERSON ET AL. 07 JUL 87 TR-51  
N00014-86-K-0316

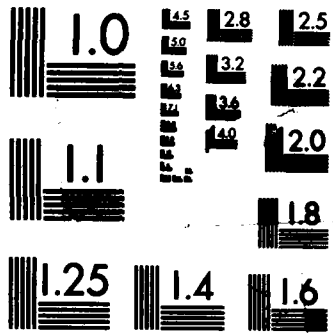
1/1

UNCLASSIFIED

F/G 9/1

NL





MICROCOPY RESOLUTION TEST CHART  
 NATIONAL BUREAU OF STANDARDS-1963-A

SECURITY CLASSIFICATION OF THIS PAGE (When Data Entered)

REPORT DOCUMENTATION PAGE		READ INSTRUCTIONS BEFORE COMPLETING FORM
1. REPORT NUMBER 51	2. GOVT ACCESSION NO.	3. RECIPIENT'S CATALOG NUMBER
4. TITLE (and Subtitle) Electro-Optical Characterization of the Tektronix TK512M-011 CCD		5. TYPE OF REPORT & PERIOD COVERED Interim
		6. PERFORMING ORG. REPORT NUMBER
7. AUTHOR(s) Patrick M. Epperson, Jonathan V. Sweedler M. Bonner Denton, Gary R. Sims, Thomas W. McCurnin and Richard S. Aikens		8. CONTRACT OR GRANT NUMBER(s) N00014-83-K-0268
9. PERFORMING ORGANIZATION NAME AND ADDRESS Department of Chemistry University of Arizona Tucson, AZ 85721		10. PROGRAM ELEMENT, PROJECT, TASK AREA & WORK UNIT NUMBERS NR 051-549
11. CONTROLLING OFFICE NAME AND ADDRESS Office of Naval Research Arlington, Virginia 22217		12. REPORT DATE July 9, 1987
		13. NUMBER OF PAGES 48
14. MONITORING AGENCY NAME & ADDRESS (if different from Controlling Office)		15. SECURITY CLASS. (of this report) Unclassified
		15a. DECLASSIFICATION/DOWNGRADING SCHEDULE
16. DISTRIBUTION STATEMENT (of this Report) This document has been approved for public release and sale; its distribution is unlimited.		
17. DISTRIBUTION STATEMENT (of the abstract entered in Block 20, if different from Report)		
18. SUPPLEMENTARY NOTES Submitted to <u>Optical Engineering</u> for publication.		
19. KEY WORDS (Continue on reverse side if necessary and identify by block number) Charge-coupled device, Charge transfer device		
20. ABSTRACT (Continue on reverse side if necessary and identify by block number) The electro-optical characterization of the first in a new series of Tektronix CCDs is described. This device, the TK512M-011, is a frontside- illuminated CCD with a 512 by 512 format and 27 by 27 micron pixels. Electro- optical characteristics measured in this study include linearity, blooming, dark count rate, charge transfer efficiency (CTE), and quantum efficiency. The results of a detailed study of the noise characteristics of the CCD out- put FET are reported. The TK512M-011 has excellent photometric linearity, high well capacity, and a low dark count rate. (Continued on other side)		

AD-A183 233

DTIC  
ELECTE  
AUG 14 1987  
S D  
AD

Very good low light level CTE is observed in the parallel shift direction however CTE problems are observed in the serial direction. The quantum efficiency of the frontside-illuminated CCD over the wavelength range of 400 to 1000 nm is reported and is lower than expected based on experience with other similar devices. The noise of the output FET of the CCD is equivalent to 5 to 12 electrons depending upon the FET operating conditions and system bandwidth. A very small latent image effect is noted. The conclusion of this evaluation is that despite the problems observed, the frontside-illuminated Tektronix CCD is an excellent sensor for scientific imaging applications.

OFFICE OF NAVAL RESEARCH  
Contract N00014-86-K-0316  
Task No. 051-549  
TECHNICAL REPORT NO. 51

Electro-Optical Characterization of the Tektronix TK512M-011 CCD

by

Patrick M. Epperson, Jonathan V. Sweedler, M. Bonner Denton,  
Gary R. Sims, Thomas W. McCurnin and Richard S. Aikens

Prepared for publication in  
Optical Engineering

Department of Chemistry  
University of Arizona  
Tucson, Arizona 85721

July 7, 1987

Accession For	
NTIS CRA&I	<input checked="" type="checkbox"/>
DTIC TAB	<input type="checkbox"/>
Unannounced Justification	<input type="checkbox"/>
By	
Distribution/	
Availability Codes	
Dist	Avail and/or Special
A-1	

Reproduction in whole or in part is permitted for  
any purpose of the United States Government.



This document has been approved for public release  
and sale; its distribution is unlimited.

## ABSTRACT

The electro-optical characterization of the first in a new series of Tektronix CCDs is described. This device, the TK512M-011, is a frontside-illuminated CCD with a 512 by 512 format and 27 by 27 micron pixels. Electro-optical characteristics measured in this study include linearity, blooming, dark count rate, charge transfer efficiency (CTE), and quantum efficiency. The results of a detailed study of the noise characteristics of the CCD output FET are reported. The TK512M-011 has excellent photometric linearity, high well capacity, and a low dark count rate. Very good low light level CTE is observed in the parallel shift direction, however CTE problems are observed in the serial direction. The quantum efficiency of the frontside-illuminated CCD over the wavelength range of 400 to 1000 nm is reported and is lower than expected based on experience with other similar devices. The noise of the output FET of the CCD is equivalent to 5 to 12 electrons depending upon the FET operating conditions and system bandwidth. A very small latent image effect is noted. The conclusion of this evaluation is that despite the problems observed, the frontside-illuminated Tektronix CCD is an excellent sensor for scientific imaging applications.

## 1. INTRODUCTION

For low light level scientific applications the charge-coupled device (CCD) is the premier electronic detector for the visible, ultraviolet, vacuum ultraviolet, and soft x-ray regions of the electromagnetic spectrum (1,2,3,4). CCD performance in terms of sensitivity, signal to noise ratio, and photometric accuracy is capable of greatly exceeding that of all other imaging detectors. Since their invention by Boyle and Smith of Bell Laboratories in 1970 (5,6), several organizations have been involved in improving the performance of CCDs in the areas of spectral coverage, readout noise, dark current, spatial resolution and charge transfer efficiency. These efforts have resulted in a class of devices termed scientific CCDs which are specifically designed to meet the needs of low light level, wide dynamic range, scientific imaging applications. Some specific areas in which needs for high resolution CCD imaging have been expressed are optical and electron microscopy, streak tube readout, high resolution multichannel optical spectroscopy, astronomical observations, surveillance, and medical and industrial radiology.

The ultimate goal of any detector for scientific imaging is to efficiently convert the incoming photon flux into a two-dimensional array of charge packets, hold the charge for the length of the observation, and then accurately measure the amount of charge present in each packet. Determining whether or not a new CCD is suitable for use as a scientific imager is done by quantifying the important physical characteristics of a CCD which determine its ability to

transduce an optical image into an electronic one with high signal to noise. Once the detector characteristics are known, the expected S/N can be estimated given the photon flux, the wavelength region, the integration time, and the noise which is present in the basic photon signal.

This paper discusses the electro-optical evaluation of the first in a family of CCDs manufactured by Tektronix which were designed for use in scientific applications (7). The detector, TK512M-011, is a 512 by 512 frontside-illuminated 3 phase CCD with 27 by 27 micron pixels. This CCD is the first in a family of devices which include both front and backside-illuminated devices in  $512^2$ ,  $1024^2$ , and  $2048^2$  two-dimensional formats. This new family of CCDs represents not only a sizeable improvement in spatial resolution available from a CCD imager, but is also predicted to provide new performance levels in terms of noise, sensitivity and dynamic range in a commercially available detector. The evaluation of the TK512M-011 centers on measuring the electro-optical properties of importance for scientific imaging.

In the evaluation of the 512 by 512 CCD, the noise performance of the on-chip amplifier is reported at several temperatures under a variety of operating conditions. The dark count rate at several temperatures, the quantum efficiency from 400 - 1000 nm, and the CTE for both the serial and parallel registers are reported. Also measured in this evaluation are linearity of response and blooming characteristics.

## 2. EXPERIMENTAL APPARATUS EMPLOYED FOR CCD EVALUATION

### 2.1 Slow-scan CCD camera system

The camera system employed for these investigations consists of a Photometrics CC180A high speed camera controller coupled to a CI181A camera head interface and a modified CH181A cryogenic camera head. The camera controller generates timing signals for the camera head interface to facilitate charge propagation, pixel readout, and other utility functions. This unit is programmed through manual input or from a host computer. A flexible command set supports operations such as subarray readout, charge binning, variable exposure time, charge clearing, and system gain control. The controller also supervises the transmission of digital intensity data to the host computer system.

The camera head interface contains the circuitry to generate CCD clock waveforms, control CCD temperature, operate an electronic shutter, perform a double correlated sample for pixel readout, and digitize pixel intensity data. To control kTC noise, a dual-slope integrator with variable integration times is used for subtraction of correlated samples before and after charge transfer to the output node. The integrator also provides electronic bandwidth control for white and  $1/f$  noise reduction. Intensity data is digitized to 14 bits precision at 50 kHz rate.

The camera head consists of a liquid nitrogen cryostat containing the CCD, preamplifier, voltage dividers, and clock signal conditioners. The CCD temperature is adjustable over the range of -50 to -120C. The temperature is regulated to  $\pm 0.5$  degrees C by a servo controlled resistive heater system. Minor modifications were made to

the camera head to facilitate external control of the CCD output FET drain voltage and current for these experiments.

## 2.2 Digital image acquisition, display, and processing system.

The system employed to acquire and analyze image data from the camera system is a Photometrics DIPS 2000 unit. This is a highly specialized computer hardware/software system designed to be used in conjunction with Photometrics slow-scan CCD cameras. The DIPS system is interfaced to the CC180A controller over a high speed DMA channel. The computer hardware of the DIPS system consists of a MC68010 processor with 1 MBYTE program RAM and 4 MByte image buffer RAM. A 65 MByte winchester disk unit with a 67 MByte formatted cartridge tape unit were used for program and image data storage. An alphanumeric/graphics console terminal was used for control and graphical data display functions. A video display memory unit was used to display images on a RS170 monitor. Hard copies of displayed images were obtained with a video hard copy unit.

Extensive image processing, analysis, and display software are supported by the DIPS system. Typical functions include linear image arithmetic functions, statistical analysis, and image display with variable contrast and spatial format.

## 3. CCD OUTPUT FET AMPLIFIER CHARACTERIZATION AND OPTIMIZATION

A CCD can be used to detect extremely faint images of less than 100 photogenerated electrons per pixel and thus must have very low noise readout amplification and digitization electronics. It is the

extremely low noise levels obtainable from CCDs which distinguish them from other solid-state and vacuum tube imagers. The low readout noise obtainable from a CCD is derived from its ability to transfer photogenerated charge to a specialized low capacitance floating diffusion which serves as the gate of the MOSFET amplifier. Readout noise levels of less than 50 electrons are quite common in CCDs, while especially superior imagers have noise levels of less than 10 electrons. The TK512M-011 was designed to have a readout noise of 2 electrons (7). Because the same amplifier is present on every device in the Tektronix CCD family, a great deal of effort was expended in carefully measuring and optimizing the performance of the on-chip preamplifier and the associated signal processing electronics.

A block diagram of the signal processing scheme used to evaluate the TK512M-011 on-chip amplifier noise characteristics is given in Fig. 1. The potential of the output node of the CCD is amplified by the on-chip FET amplifier. The signal from this FET amplifier is further processed by additional gain, dc restoration circuitry and a double correlated sampling process. Conversion to a digital format is accomplished by a sample-hold and an analog-to-digital converter. The optimum operating point and the noise performance of the CCD output FET were investigated in detail.

Optimization of the CCD output FET signal-to-noise ratio required

- (a) determining the voltage gain and output impedance of the device,
- (b) determining the output noise from the device and then combining
- (a) and (b) into an overall figure-of-merit. Given the FET output

noise, and an output signal (assumed noiseless) the output signal-to-noise ratio is given by:

$$S/N = (\text{output signal power})/(\text{output noise power}). \quad (1)$$

The following development assumes that the output noise can be adequately represented by a flat spectral density modified by a filter function. This assumption is justified by the low corner frequency of the observed  $1/f$  noise from the device, the double-correlated sample procedure, and the high pass filtering used in the preamplifier. Since both signal and noise appear across the same output impedance, the output signal-to-noise ratio is

$$S/N = ([S_n * G]^2) / ([E_n]^2 * BW), \quad (2)$$

where  $S_n$  is the input signal expressed in volts rms,  $G$  is the device voltage gain from input to output,  $E_n$  is the device noise spectral density expressed in volts rms across the device output impedance and  $BW$  is the noise bandwidth of the fixed filter function in Hz.

The following decibel measure based on one volt across the output impedance (dbv) is a monotonic function for positive arguments and is used as a basis for a figure-of-merit:

$$S/N_{\text{dbv}} = 20\log(S_n) + 20\log(G) - 20\log(E_n) - 10\log(BW). \quad (3)$$

The input signal level is arbitrary and can be kept constant for figure of merit determination. The output filter noise bandwidth is a constant for a given setup of the double correlated sampling. Therefore, the figure-of-merit (FOM) used in these studies is

$$\text{FOM}_{\text{dbv}} = 20\log(G) - 20\log(E_n). \quad (4)$$

Maximizing the above function is equivalent to maximizing the output signal-to-noise ratio from the device for a fixed sense node capacitance.

The output FET was characterized using a curve tracer (Fig. 2) to determine incremental forward transconductance,  $g_{fs}$ , using the relationship:

$$g_{fs} = (\Delta I_{ds}) / (\Delta V_{gs}). \quad (5)$$

Given the incremental transconductance, a source resistor  $R_s$ , and a simple FET follower model, the gain and output impedance,  $R_{out}$ , of a source follower circuit are

$$\text{Gain} = (g_{fs} * R_s) / (1 + [g_{fs} * R_s]), \quad (6)$$

$$R_{out} = R_s / (1 + [g_{fs} * R_s]). \quad (7)$$

Output noise from the CCD output FET was measured using a carefully calibrated spectrum analyzer. The results showed a relatively flat spectral density plus a low-frequency  $1/f$  region. At good operating points the corner frequency of the  $1/f$  region was well below 10 kHz. The  $1/f$  region did extend far enough to affect the estimated noise output from the double correlated sampling at several operating points of the FET; however, these points occurred at relatively high overall noise values and did not represent optimum device operating conditions.

Noise data were taken and the forward transconductance determined at a number of operating points at +21, -80, -100, -120, and -130 degrees C. The output FET drain voltage ( $V_d$ ) was varied from 8 to 22

volts. FET source current was varied from 0.3 milliamperes to approximately 0.8 milliamperes. The reset FET drain voltage ( $V_g$ ) was varied from 2 to 15 volts. The FET noise was measured for over 100 different combinations of operating conditions.

The data were interpreted as follows. Using the measured FET incremental forward transconductance values, the source follower gain and output resistance were computed for each operating point. Optimum operating points as functions of temperature were then determined using Eq. (3). A typical analyzed data set is summarized in Table 1. The equivalent noise in  $\text{nv}/\sqrt{\text{Hz}}$  at the output FET as measured on a spectrum analyzer in the flat portion of the spectrum is included in Table 1. The noise was converted to equivalent electrons assuming a CCD gain of 0.7 microvolts/electron and the full bandwidth of the double correlated sampler.

The CCD output FET as tested supports operation at device noise levels of approximately five electrons rms using sampling integration times as short as 4.2 microseconds. Lower equivalent noise levels could be realized with longer sampling integration times. We have designed an off-chip pre-amplifier whose noise is compatible with the noise characteristics of the device using readily available components.

A number of good CCD FET operating points were found at all of the cooled temperatures. In some cases at room temperature excess low frequency noise was observed that increased with drain to source voltage. This condition was observed at the onset of surface channel

operation of the FET at device currents exceeding 0.5 milliamperes, and for drain to source voltages exceeding approximately 5 volts.

The total noise observed at the preamplifier output is dominated by Johnson noise associated with the output impedance of the CCD output FET follower. This noise source can only be improved by increasing the transconductance of the output FET. Finally, it must be noted that all results reported are from measurements on a single CCD.

#### 4. DEVICE RESPONSE LINEARITY MEASUREMENTS

The linearity of the TK512M-011 CCD and associated analog to digital electronics was measured. The apparatus employed for linearity measurements consists of a ring of red light emitting diodes (LEDs) and several light diffuser screens used to allow the LEDs to evenly illuminate a large portion of the CCD. The flash duration of the LEDs is computer controlled to millisecond intervals with a reproducibility of 10 nanoseconds. In order to avoid the effects of junction heating on the light output of the LEDs, the LEDs were flashed for one millisecond followed by a cool down time of 20 milliseconds. The measurements were started by flashing the LEDs many times to allow them to reach a steady temperature. The amount of light reaching the detector was accurately and reproducibly controlled by flashing the LEDs the desired number of times.

The linearity measurement involves using a series of uniformly increasing exposures and plotting the observed mean signal measured in

a subarray of the CCD as a function of illumination level. The results are shown in Fig. 3 for exposures of zero to over  $3 \times 10^5 e^-$ ; this is the range of the 14 bit analog-to-digital converter with the gain set so that the system noise is roughly equivalent to the least significant bit. A close examination of this figure will reveal a slight deviation from a linear response. The largest deviation from a linear least squares line fit to the data in Fig. 3 was approximately 100  $e^-$ . These deviations divided by the response at highest illumination level measured ( $3 \times 10^5 e^-/\text{detector element}$ ), give a relative maximum deviation from a linear response of 0.03%.

##### 5. THERMAL CHARGE GENERATION MEASUREMENTS

While the decrease in the CTE performance of the CCD at low temperatures defines the lower temperature limit of operation, the upper temperature limit is set by the rate of thermal generation of charge and the longest integration time which will be used. One of the major uses of the TK512 series of CCDs is astronomical imaging involving long exposures; therefore, a detailed knowledge of the rate of thermal charge generation is important. If the thermal charge generation rate cannot be sufficiently reduced by cooling, then the shot noise present on the thermally generated charge for long exposures limits the minimum detectable signal. The thermal generation of charge, often called dark current, is due to electron-hole pair generation by midgap defects in the bulk semiconductor and

at the Si-SiO<sub>2</sub> interface (8). The most significant source of dark current is from surface state defects at the Si-SiO<sub>2</sub> interface (9).

The thermal generation of charge was determined by taking long integration time dark exposures and finding the mean value of a subarray. With integration times of many minutes, cosmic ray events and background radiation become significant and can limit the longest integration times possible with this detector. The dark current at 142 K with a 2000 second integration time for the TK512M-011 was measured to be 56 electrons (0.03 electrons/second), and thus introduces less than eight electrons of noise. Fig. 4 shows the dark counts per detector element per second observed at several temperatures between 298 K and 140 K. Using this figure, the dark count rate can be estimated for any desired temperature in this range. Although the thermal charge generation rate for this CCD is low enough for most applications, the thermal generation rate is about an order of magnitude higher than reported for other CCD detectors (1,10).

It may be possible to reduce the dark count rate of this device further by adjusting the parallel clock potentials. For a similar CCD, lowering the lower parallel clock voltage during integration to form an inversion layer under the parallel gate electrodes decreased the dark count rate more than an order of magnitude by suppressing thermal generation of charge from surface interface states (9). To minimize the dark count rate as well as reduce the residual image, all three phases should be biased to form an inversion layer, with potential barriers between individual detector sites maintained by irregularities in the potential wells. While reducing the dark

current, this also reduces the full well capacity of the individual detector sites and so a compromise must be made depending on the particular application. Currently, this technique of dark count reduction is being evaluated for the TK512M CCD.

## 6. SPECTRAL RESPONSE MEASUREMENTS

The sensitivity of a CCD sensor at any given wavelength is one of the most important parameters when a particular device is being considered for a specific scientific imaging application. For this reason a large effort was expended to accurately measure the quantum efficiency (charge carriers collected and measured per incident photon) of the TK512M-011 CCD as a function of wavelength over the near IR to ultraviolet range. These measurements were accomplished by determining the quantity of charge generated in a subarray of the detector during a known integration period due to photons from a monochromatic source of known flux and wavelength.

The sensitivity of a CCD at any wavelength is strongly affected by the optical properties of the silicon epitaxy, the overlaying gate electrodes and the silicon dioxide layers. The sensitivity of all CCDs decreases in the near IR due to a number of factors including the decreasing absorption coefficient of silicon at longer wavelengths. As the absorption coefficient decreases, photons are either absorbed deep in the epitaxy or pass entirely through the epitaxy and are absorbed in the bulk silicon. For devices with 10 micron epitaxy layers, 90% of 1000 nm radiation passes through the epitaxy (11).

Silicon CCDs do not respond to photons corresponding to energies less than the band gap of silicon (approximately 1.1 eV at 300 K). Frontside illuminated polyphase charge coupled devices constructed with processes and structures similar to the TK512M-011 typically exhibit very low quantum efficiencies in the blue-visible and ultraviolet wavelengths. This is primarily due to photon absorption and reflection from the multiple polysilicon electrodes (1,12).

The quantum efficiency measurements on the TK512M CCD are reported for the wavelength range of 400-1000 nm. A 0.35 meter f/6.8 Czerny-Turner monochromator with a 1080 line/mm grating blazed at 250 nm was used for wavelength dispersion. In order to have sufficient throughput for flux determinations, it was necessary to open the entrance and exit slits of the monochromator to 2.0 mm so that the spectral bandpass was 4.0 nm. The output of the monochromator was directed into the input port of a four inch integrating sphere which created uniform illumination of the detector. Band pass and long pass filters were used as necessary to prevent stray light and second order radiation from reaching the detector. A computer controlled electronic shutter was used to precisely control the exposure times for the CCD. An EG&G photodiode with a calibration traceable to the National Bureau of Standards was employed with a calibrated picoammeter to measure the photon flux exiting the integrating sphere/cm<sup>2</sup> as a function of wavelength at a precisely known distance from the exit port. An anti-reflection coated fused silica window similar to the one used in the CCD camera cryostat was placed in the

optical path between the integrating sphere and the photodiode to compensate for reflection of this element.

To complete the quantum efficiency measurements, the photodiode was removed from the apparatus and the CCD sensor head attached so that the surface of the detector was at the same distance from the exit port of the integrating sphere. The quantity of charge generated in a subarray of the CCD during a known integration period was determined at the same wavelengths that flux measurements were made. The mean signal was computed and multiplied by the system gain to determine the number of photoelectrons collected. By normalizing the photoactive areas of both detectors and correcting for the quantum efficiency of the photodiode, the quantum efficiency of the CCD as a function of wavelength was calculated. The quantum efficiency measurements on the frontside CCDs were repeated three times using one device to test precision. A second device was tested to verify uniformity between devices. The accuracy of the QE apparatus was further confirmed by measuring the quantum efficiency of CCDs from RCA and Texas Instruments and comparing the results with literature values.

The results of the quantum efficiency measurements for the TK512M-011 CCD are shown in Fig. 5. The quantum efficiency of the frontside Tektronix CCD is fairly low when compared to other multiphase frontside-illuminated CCDs such as the Thomson TH7861 (13). The peak quantum efficiency for the devices tested occurs at 35% at 750 nm. The value drops to 3% at 400 nm and 1% at 1000 nm. The sharp variations in sensitivity are typical of the interference effects of

the gate electrodes seen in frontside-illuminated CCDs when illuminated with narrow band light.

While the measured quantum efficiency of the frontside imager is lower than the literature suggests (7), the device still has a significant response in the 450 to 900 nm spectral range. It should be noted that in the quantum efficiency measurements described for the frontside imager, the CCD was maintained at low temperatures. The quantum efficiency of the CCD in the near IR can be increased by operating the device at higher temperatures. While the increase is expected to be only a few percent at 800nm, it is likely the quantum efficiency at 1000 nm can be increased several fold (14).

#### 7. CHARGE TRANSFER EFFICIENCY MEASUREMENTS

Charge transfer efficiency (CTE) of the CCD was measured at low charge levels by the method of illuminating the CCD with low energy x-rays from an Fe <sup>55</sup> radioactive source developed by Janesick et al (1). CTE is generally dependent upon parallel and serial clock levels, the temperature of the CCD, and the amount of charge being transferred. The most serious limitation to achieving high CTE in low light images is the loss of charge to what is termed the "spurious potential pocket" (15,1). The amount of charge trapped is a small fraction of full well, therefore smearing is apparent only at very low light levels.

Because of the large number of transfers in a 512 by 512, 3 phase CCD, CTE values near unity are necessary to avoid any significant

smearing of the image. Fig. 6 illustrates the path that a particular charge packet takes during charge readout. The transfer process is divided into those which move charge in the parallel shift direction and those which move charge in the serial shift direction. The overall parallel transfer of charge is further divided into the CTE associated with transfer of charge in the imaging region and the CTE associated with the transfer of charge from underneath the last parallel gate to the serial register. This distinction is necessary because of the different gate structure present in the Tektronix CCD used to transfer charge from the last parallel gate to the serial register. The number of parallel transfers each charge packet may take is dependent upon its distance from the serial register. Referring to Fig. 6, for a charge packet located at element Z with coordinates x and y, the overall parallel CTE is;

$$CTE_{\text{parallel}} = CTE_{p \rightarrow s} * CTE_p^{3y}, \quad (8)$$

where  $CTE_{p \rightarrow s}$  is the CTE associated with the parallel to serial transfer step, and  $CTE_p$  is the CTE of the parallel region. The factor of 3 is for the 3 transfers of charge in a 3 phase device when moving charge from one pixel to the next. The equation describing the overall serial CTE is;

$$CTE_{\text{serial}} = CTE_{s \rightarrow sw} * CTE_s^{3(x + 50)}, \quad (9)$$

where  $CTE_{s \rightarrow sw}$  is the CTE associated with the transfer between the last serial gate and the output summing well,  $CTE_s$  is the average CTE of charge transfer in the serial register. The 50 accounts for the

extra 50 elements added to the serial register to separate the output amplifier from the gates of the image area. Both Eqs. (8) and (9) include a position dependent and position independent component which can be distinguished qualitatively from each other by visual inspection of an image. For example, in an image with poor parallel CTE, trailing of charge which increases as a function of distance from the serial register is indicative of a problem with the CTE of the parallel region. However, for images where the trailing of charge in the parallel direction is constant across the CCD, the cause of poor CTE is the single charge transfer step from the parallel to serial region.

Ideally, if the electron cloud from the absorption of an x-ray is always collected in one detector element with no lateral diffusion and readout with unity charge transfer efficiency, the image would be a single point with no charge in adjacent elements. However, because the electron cloud is not always collected in a single potential well, the charge will be distributed among adjacent elements. On the average, the amount of charge should initially be equal in the elements which precede and trail the x-ray peak. During readout, some charge in the x-ray peak is left behind and accumulates in the trailing elements, thus the trailing pixel has slightly more charge than the pixel preceding the x-ray peak. The amount of asymmetry in the image of the x-ray absorption is an indication of the charge transfer efficiency from preceding to following elements. By measuring the amount of trailing from x-rays in both directions from

different areas of the CCD, values of CTE for the various transfer steps in the CCD are extracted.

CTE was measured at the moderately low charge level of 1620 e- using an Fe<sup>55</sup> radioactive source which emits 5.9 Kev Mn K-alpha x-rays. The source is mounted in a steel cylinder and rod assembly as shown in Fig. 7, which allows positioning the source 1 to 250 mm from the CCD surface. By changing the x-ray source to CCD distance the x-ray flux can be conveniently adjusted. CTE was determined by measuring the trailing of charge from detector elements which had absorbed an x-ray. For each 2 second exposure to the Fe<sup>55</sup> source, x-ray events were identified and their location, intensity, and the intensity of detector elements adjacent to it in both the serial and parallel transfer direction were recorded. A total of 64 exposures were taken in order to acquire enough events to calculate CTE. The identification of x-ray events was accomplished by searching for pixels whose intensity ranged between 50 to 100 % of the maximum charge possible from the complete absorption of a 5.9 Kev x-ray. Detector elements adjacent to pixels which satisfied the above condition were limited to values between -5 to 25 % of the total charge possible from one x-ray. Limiting the x-ray events to those which satisfied the above two conditions was designed to restrict the data to x-ray events where most of the electron cloud was collected by a single detector element. This screening helped to simplify the CTE analysis and improve the overall accuracy of the CTE measurement. Only small subarrays of the CCD were read to keep the readout time short compared to the integration time. The location of the subarray

was moved to each corner of the CCD in order to realize both the maximum and minimum number of transfers in both the serial and parallel shift directions.

CTE values which describe the average parallel and serial transfer of charge are shown in Table 2 as a function of temperature. CTE in both the serial and parallel directions tends to degrade as the temperature is lowered. The parallel CTE is excellent and results in images which have no discernible streaking of charge in the parallel shift direction. The serial CTE is quite poor and causes streaking in the serial direction even from the corner of the CCD nearest the output amplifier as seen in Fig. 8. This behaviour indicates that there is poor charge transfer between the last serial element and the summing well of the output amplifier.

## 8. BLOOMING MEASUREMENTS

Onset of blooming in a CCD occurs when the maximum number of photogenerated charge carriers which can be collected in one detector element and transferred to the floating diffusion of the output amplifier is exceeded. Because of the unique readout mode of a two-dimensional CCD, charge initially generated in the image region is transferred through several different regions before being sensed at the output node, and thus blooming can occur in several different areas.

Blooming measurements are important in determining the device performance at high illumination levels. For example, when using a

CCD as a detector at the focal plane of a spectrograph, blooming is a serious and sometimes limiting factor in measuring spectra with both intense and weak spectral lines (12). Blooming effects can be minimized by orienting the spectral lines in the parallel shift direction, such that if blooming occurs it will happen along the direction of the slit and not in the direction of wavelength dispersion. The above technique is effective only if the charge capacity of the serial register is equal to or larger than the parallel register, as is usually the case for most CCDs.

To measure the blooming in the three regions of the CCD, a point source of visible light was imaged onto a detector element and its response and the response of adjacent detector elements as a function of illumination level were monitored. Blooming was determined by noting the illumination level at which any detector element showed a sudden increase in signal caused by charge spilling into it from an adjacent oversaturated detector element. Monitoring the response of the adjacent elements in addition to the central element is important for two reasons. First, it provides a more accurate estimate of blooming onset than simply measuring the saturation point of the brightest element. When the majority of light is focused onto a single central element, the rate of increase of an adjacent pixel is much sharper than the rolloff of the central element's response at the onset of saturation. Second, by monitoring the response of adjacent elements in both the serial and parallel shift direction, the direction of charge blooming is determined.

The light source was a 25 micron pinhole illuminated with 600 nm light focused onto the CCD with a 50 mm f/2 lens and a #3 extension tube. The gain of the analog to digital electronics was decreased for blooming measurements to 64 electrons /ADU while measuring blooming in the serial and parallel registers, and 640 electrons/ADU while measuring the summing well capacity. In order to measure the serial register and the summing well blooming, charge binning was used to transfer a sufficient amount of charge into each well without being limited by the well capacity of a previous region of the CCD. For example, in order to measure the blooming caused by exceeding the charge capacity of the summing well, a larger defocussed pinhole image was binned 32 fold in both the serial and parallel shift directions. Therefore each element of this binned image was composed of the charge from 1024 pixels. The ability to combine charge at the summing well made it possible to isolate and measure the much larger summing well capacity. In a similar fashion, charge from several pinhole images was binned into the serial register in order to isolate and quantitate blooming in the serial register.

The response from a typical blooming measurement is plotted in Fig. 9 and describes the response of the central and four adjacent detector elements as a function of illumination level of the central element. Note the response of the central pixel Z saturated at the same illumination level as the the response of a pixel adjacent to Z showed a sudden increase in slope (in this case indicating blooming in the parallel register). Results of the blooming measurements of the Tektronix 512M-011 are listed in Table 3. As expected, the onset of

blooming depends strongly upon gate potentials, increasing as the upper gate potentials are raised. The summing well saturates at  $6.2 \times 10^6$  electrons, beyond which charge can no longer be binned into the summing well and spills back into the serial register. A charge storage capacity of this magnitude along with a read noise of 6 electrons yields a dynamic range of greater than  $10^6$  when using this CCD in a highly binned readout mode.

Blooming usually occurred in the serial register before the parallel register for most of the gate voltages investigated. The maximum amount of charge which could be contained in the serial register before blooming occurred was 940,000 electrons, and occurred at the maximum serial clock voltage swing of -8 to +12 volts. Blooming in the parallel register was difficult to measure at most clock levels investigated for two reasons. The first is that charge first bloomed in the serial direction, rather than the parallel direction for most clock voltages for this particular CCD. Blooming in the parallel register was determined by going past the point at which the central element bloomed in the serial direction until the device bloomed into pixels adjacent to the central element in the parallel direction. The second problem with measuring parallel register blooming was that when the high parallel clock level exceeded +5 volts, and the charge in any pixel reached 400,000 electrons, streaking occurred in the serial direction. The streaks began immediately after the bright pixel with the intensity showing an exponential decay in the serial direction. The smearing of bright detector elements disappeared when the high parallel clock was reduced

to below +5 volts and was insensitive to the serial clock voltage levels. It is believed that this effect is due to a small pocket of charge trapped in the parallel to serial transfer region which bleeds into trailing pixels when charge in the serial register is clocked out.

The optimum gate voltages for this particular Tektronix CCD based only on these blooming measurements were arrived at by maximizing the serial and parallel full wells without exceeding the clock voltages that caused the parallel to serial transfer gate smearing of charge. At these clock levels blooming in the serial and parallel directions occurs at approximately the same charge levels and no smearing of bright pixels in the serial shift direction is observed. It should be noted that these measurements were made on a single CCD. According to Tektronix, the gate area devoted to the serial register was designed to give the serial register twice the full well of the parallel register. The fact that blooming in the serial register occurs at charge levels equal or less than the level which causes blooming in the parallel registers and that the serial CTE is poor indicate that either charge is not being properly contained in the serial register potential wells or that charge is not being efficiently transferred from the serial register into the output summing well.

#### 9. LATENT IMAGE OBSERVATIONS

During initial investigations into the imaging properties of the TK512-011 frontside-illuminated CCD, an effect was observed in which a

previously recorded image would reappear to a small degree in a later readout. Several qualitative experiments were conducted to attempt to understand the mechanism of this effect. In a typical experiment, the CCD was operated in the slow-scan camera cooled to  $-100^{\circ}\text{C}$ . A test pattern illuminated with 800 nm radiation was imaged on the CCD until the highlight areas were at approximately 1/4 full well. The shutter was closed and the CCD was read out, then immediately read out again. In the second read, there was no evidence of a latent image. Next, the CCD was allowed to integrate charge in the dark for 60 seconds, then read out a third time. In this read, a latent image identical to the test pattern with approximately 7 electrons RMS in the highlight areas was observed.

Latent image effects have been observed to varying degrees of severity in all Tektronix frontside illuminated CCDs characterized in these laboratories. This effect has also been observed by other investigators.\*\* This phenomenon can arise from two possible mechanisms: charge arising from interface states at the  $\text{Si-SiO}_2$  interface, and charge arising from defects in the epitaxy-substrate junction. Charge trapped in either of these interfaces will slowly be released back into the conduction band. Any released charge which is subsequently accumulated in the potential wells of the imaging array contribute to a latent image.

These mechanisms account for the observation that latent images do not appear immediately after a high level image is read, but "grow" slowly as the CCD integrates charge. The rate of release from the trap zone is very slow at  $-100^{\circ}\text{C}$  as latent image generation has been

observed to persist for many minutes after initiation. The second mechanism accounts for the observation that long wavelength photons are necessary to initiate a latent image. Only longer wavelengths can penetrate deep enough to generate charge near the epitaxy-substrate junction.

\*\* Footnote 1. J.R. Janesick, JPL and Harry Marsh, Tektronix, personal communications.

## 10. CONCLUSIONS

The evaluation of the TEK512M-011 frontside-illuminated 512 by 512 element CCD shows it to be a promising detector for scientific applications. Table 4 is a summary of these evaluation results. The output FET exhibits a noise floor equivalent to 5 to 12 electrons depending on the integration time of the dual slope analog processor. Additionally, the optimal FET operating conditions are not critical functions of temperature, drain to source voltage or drain current. The electro-optical characterization reveals extraordinary performance in many respects, as well as several problems in the device which need improvement. Very good low light level CTE is observed in the parallel shift register. However, poor serial CTE is observed in the serial direction partially due to difficulties in transferring charge to the output amplifier. The quantum efficiency observed for this device is lower than expected. Finally, a extremely slight latent image effect is observed under certain conditions. Some of the

encouraging characteristics of the device tested are excellent linearity, very high dynamic range, and low dark current. In general, the TK512M-011 has the potential to be an excellent scientific image sensor.

It is important to realize that these results are from the characterization of a limited number of preliminary CCDs. It is expected that in the near future, devices will be available with significantly improved electro-optical characteristics. The evaluation of the frontside illuminated TK512M-011 CCD has importance to the larger CCD arrays being introduced by Tektronix. These devices have the same FET preamplifiers and same geometry detector elements, thus many of the results of the evaluation of the  $512^2$  CCD will apply to the  $1024^2$  and  $2048^2$  format CCDs. Initial work in these laboratories with a  $2048^2$  device indicates great similarities in operating conditions and imaging performance between the two detectors.

The introduction by Tektronix of an entire line of CCDs designed exclusively for scientific applications has great importance for the scientific CCD imaging community. The demand for CCD imaging systems for scientific use is increasing rapidly, while the number of manufacturers of commercial scientific grade CCDs is decreasing. The continued availability of commercial CCDs rests with the introduction of CCD sensors by such companies as Tektronix, Reticon, Thomson-CSF, and Kodak.

## 11. ACKNOWLEDGMENTS

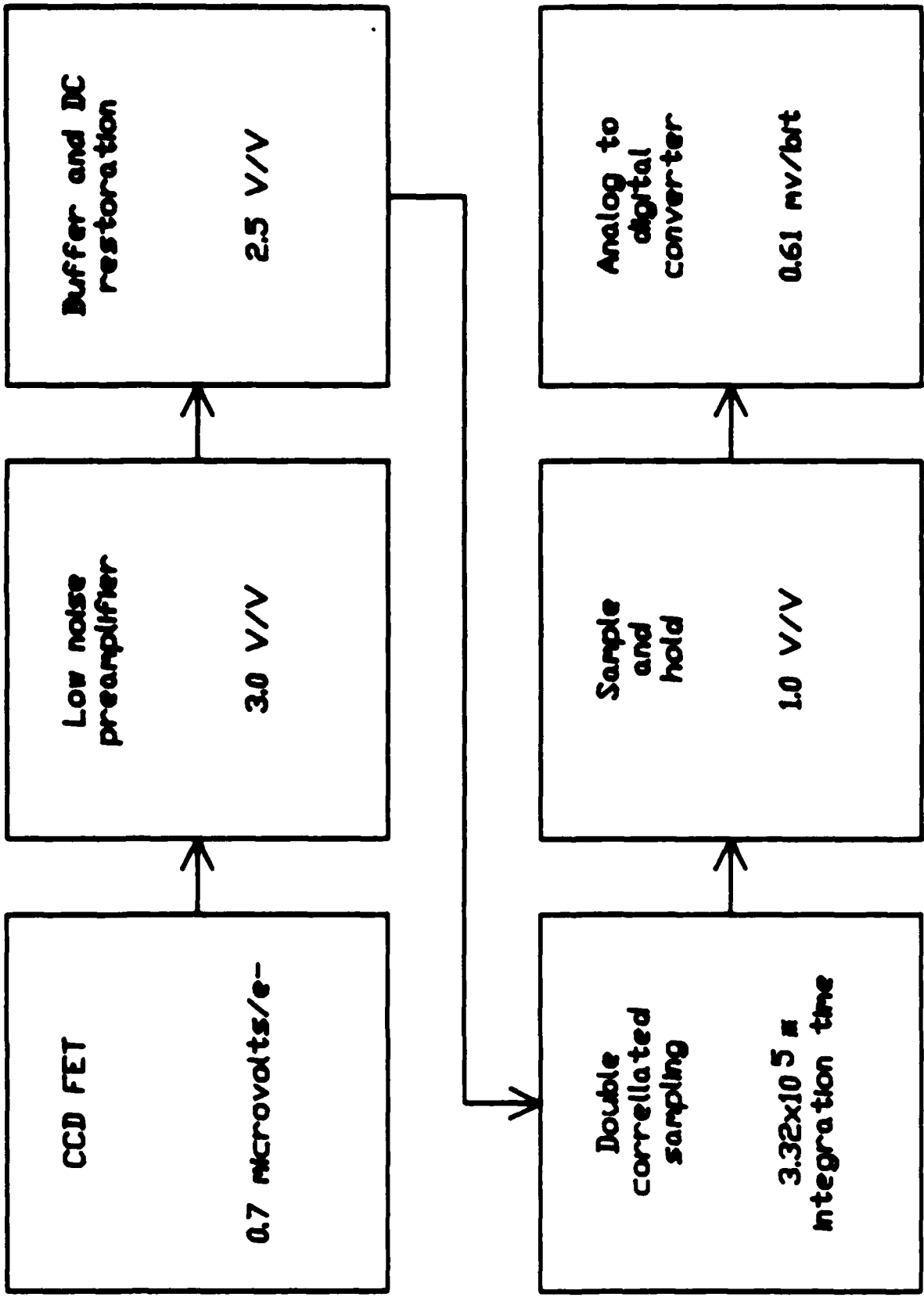
The research reported in this paper was partially funded by the National Aeronautics and Space Administration (Contract No. NAS 5-29284) and the Office of Naval Research. We wish to thank Jack Orach and Keith Copeland for assistance in the design and construction of the CCD test fixtures.

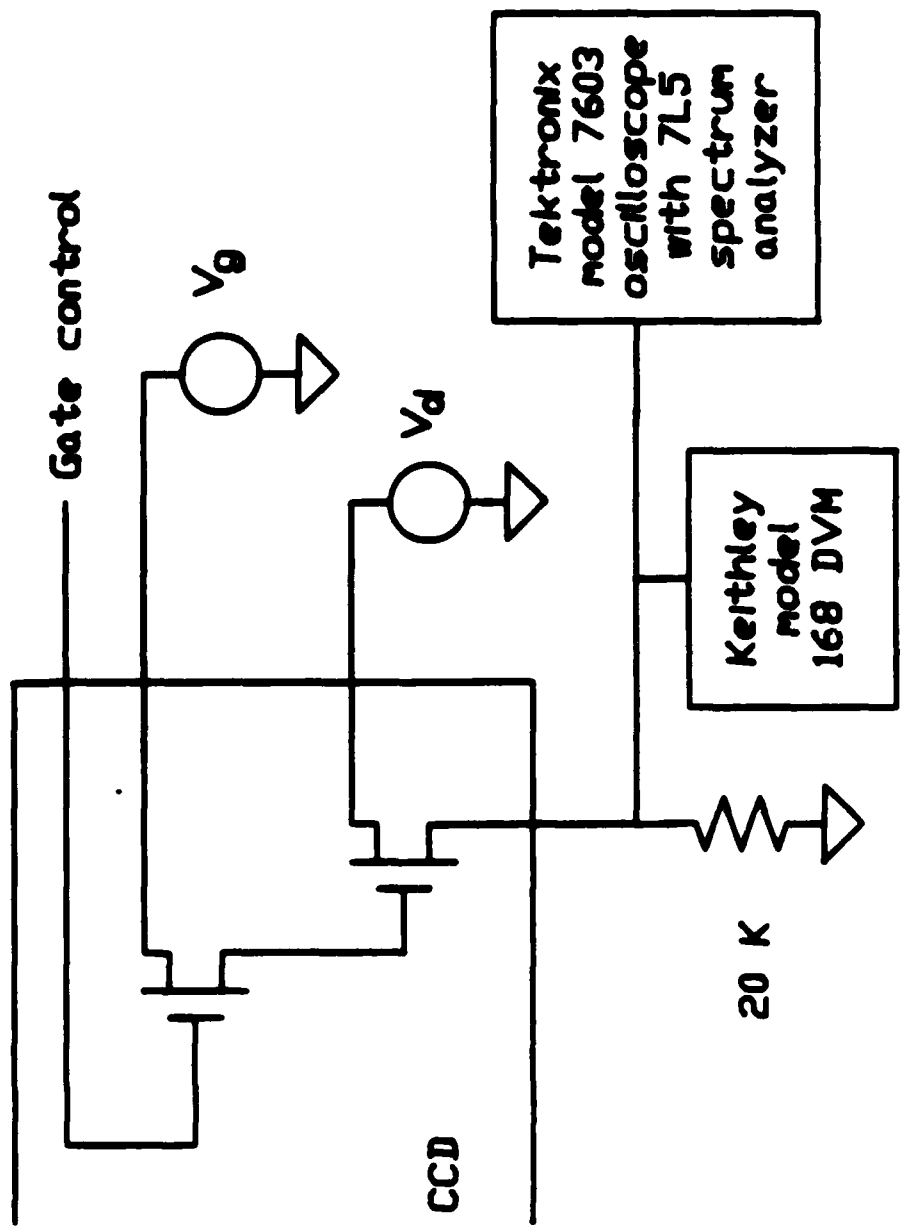
## 12. REFERENCES 1 to 15

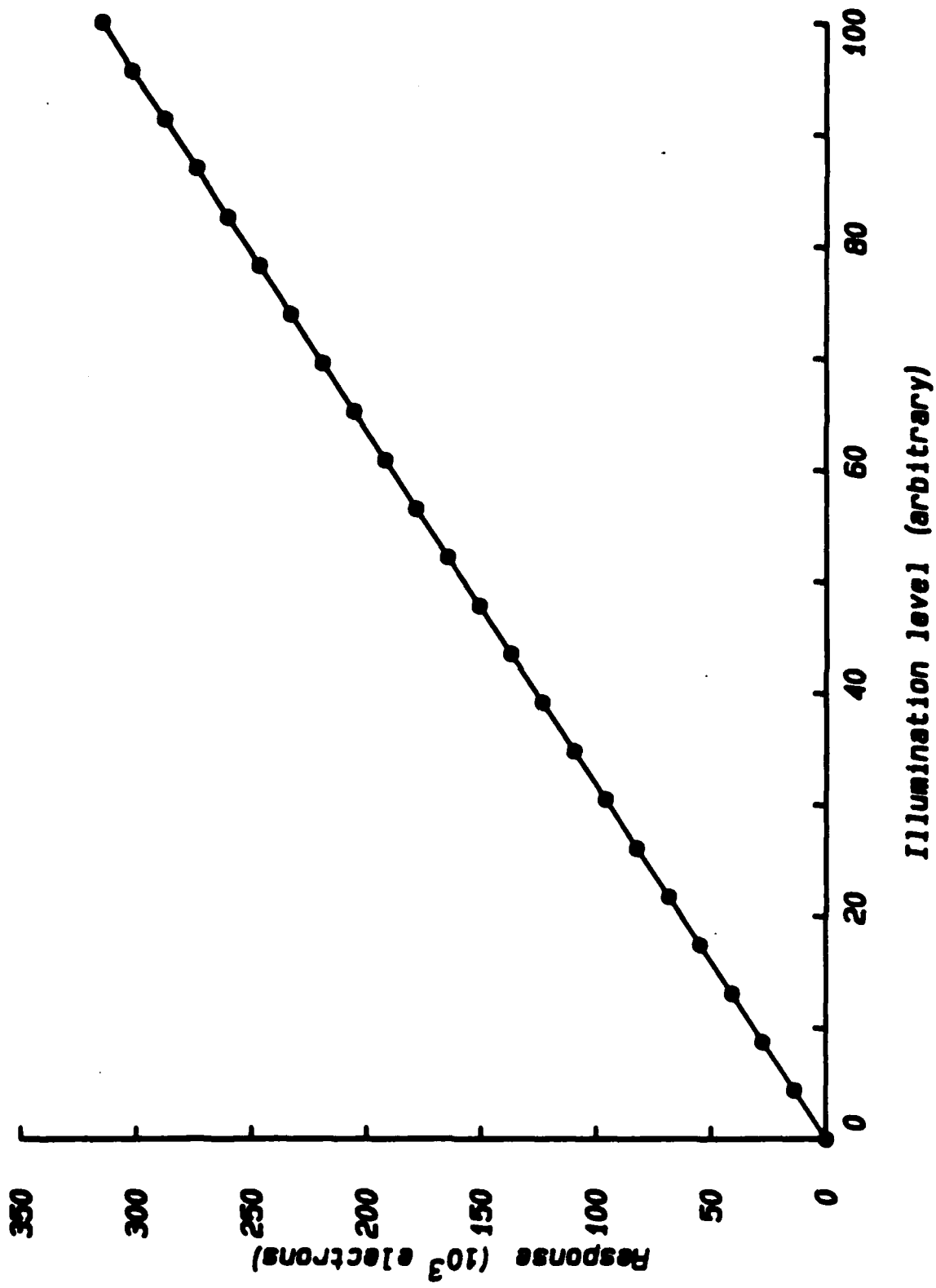
- 1) J. Janesick, T. Elliott, S. Collins, H. Marsh, M. Blouke, and J. Freeman, "The future scientific CCD," in State-of-the-Art Imaging Arrays and Their Applications, K. Prettyjohns, ed., Proc. SPIE 501, 2-31 (1984).
- 2) J. B. Oke, "Low and moderate resolution spectroscopy with an RCA charge-coupled device (CCD)," in Solid State Imagers for Astronomy, J. Geary and D. Latham, eds., Proc. SPIE 290, 45-50 (1981).
- 3) J. Janesick, D. Campbell, T. Elliott, T. Daud, P. Ottley, "Flash technology for CCD imaging in the UV," in UV Technology, R. Huffman, ed., Proc. SPIE 687, 36-55 (1986).
4. A. Fowler, P. Waddel, L. Mortara, "Evaluation of the RCA 512X320 charge-coupled device (CCD) imagers for astronomical use," in Solid State Imagers for Astronomy, J. Geary and D. Latham, eds., Proc. SPIE 290, 34-44 (1981).
- 5) W. S. Boyle, G. E. Smith, "Charge Coupled Semiconductor Devices," Bell System Tech Journal 49, 587-593 (1970).
6. G. F. Amelio, M. F. Tompsett, G. E. Smith, "Experimental Verification of the Charge Coupled Device Concept," Bell System Technical Journal 49, 593-600 (1970).

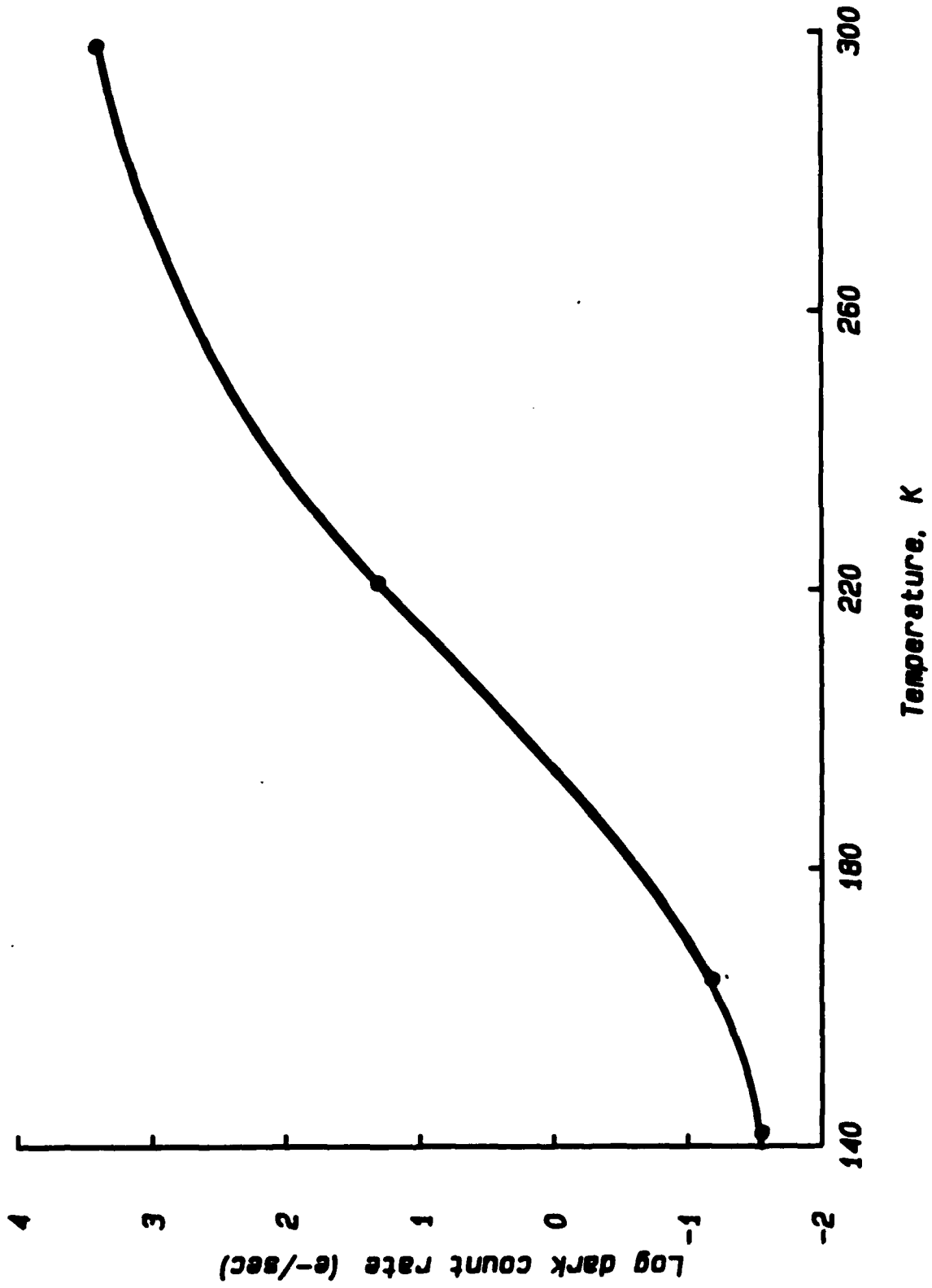
- 7) M. M. Blouke, D. L. Heidtmann, B. Corrie, M. L. Lust, J. R. Janesick, "Large area ccd image sensors for scientific applications", in Solid State Imaging Arrays, K. Prettyjohns, E. Dereniak, eds., Proc. SPIE 570, 82-88 (1985).
- 8) N. S. Saks, "Interface state trapping and dark current generation in buried channel charge-coupled devices", J. Appl. Phys. 53(3), 1745-1753, (1982).
- 9) N.S. Saks, "A Technique for suppressing dark current generated by interface states in buried channel CCD imagers", IEEE Electron Device Letters, EDL-1(7), 131-133, (1980).
- 10) M. Blouke, J. Janesick, J. Hall, and M. Cowens, "Texas Instruments (TI) 800X800 charge-coupled device (CCD) image sensor", in Solid State Imagers for Astronomy, J. Geary and D. Latham, eds., Proc. SPIE 290, 6-15 (1981).
- 11) EEV Technical Note 1(1), "Basic Operation of a CCD Frame Transfer Array", (1982), Essex, England.
- 12) M. B. Denton, H. A. Lewis, and G. R. Sims, "Charge-injection and charge-coupled devices in practical chemical analysis," in Multichannel Image Detectors, ACS Symposium Series, Y. Talmi Ed., 2, 133-154 (1983).

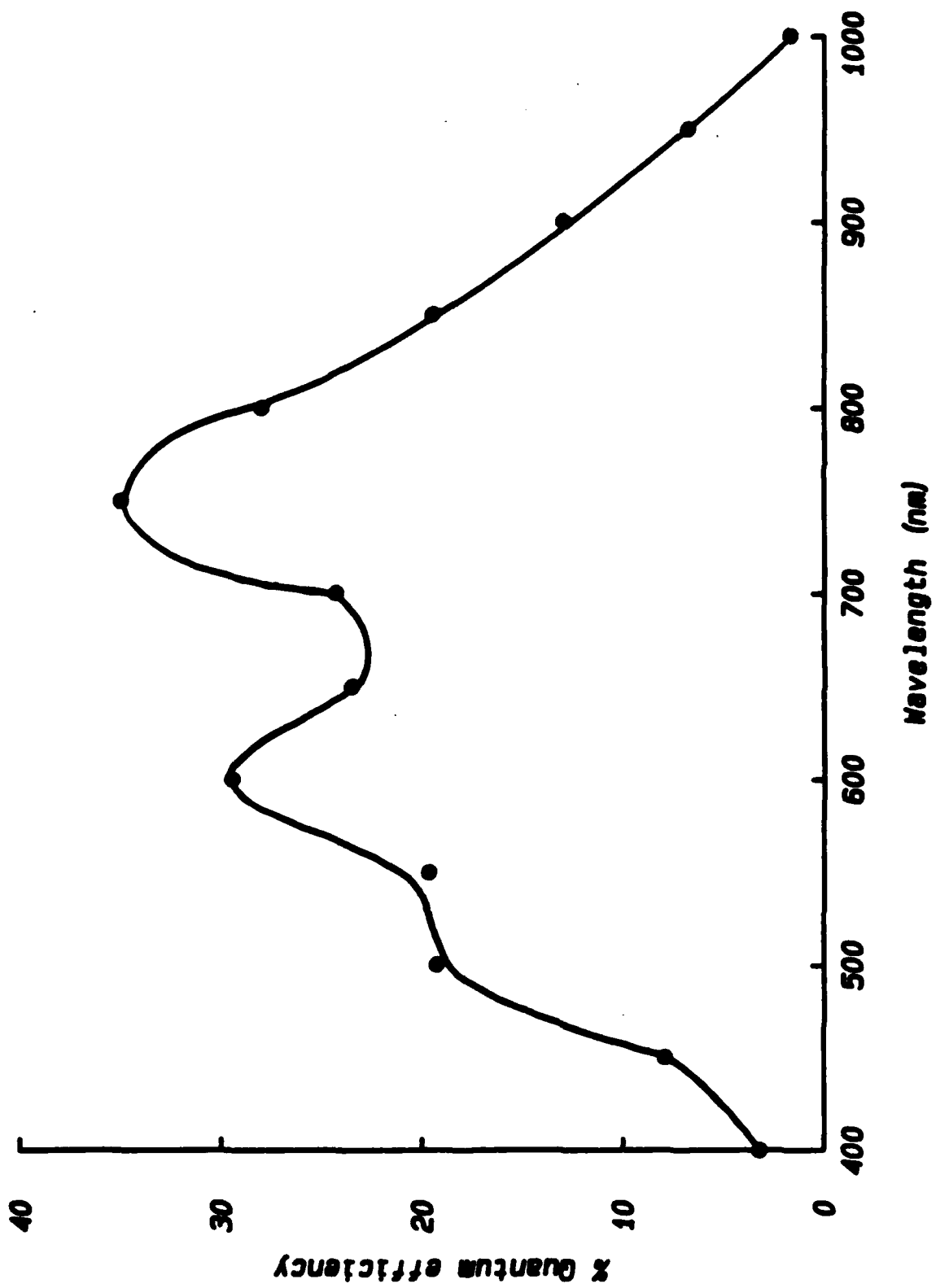
- 13) TH7861 Data Sheet, Thomson-CSF, Cedex, France, (1983).
- 14) S. Vogt, R. Tull, P. Kelton, "Self-scanned photodiode array: high performance operation in high dispersion astronomical spectrophotometry," Applied Optics 17, 574-592 (1978).
- 15) J. Janesick, T. Elliott, S. Collins, T. Daud, D. Cambell, A. Dingizian, G. Barriere, "CCD advances for X-ray scientific measurements in 1985," in X-ray Instrumentation for Astronomy, J. Culhane, ed., Proc. SPIE 597, 364-380 (1985).

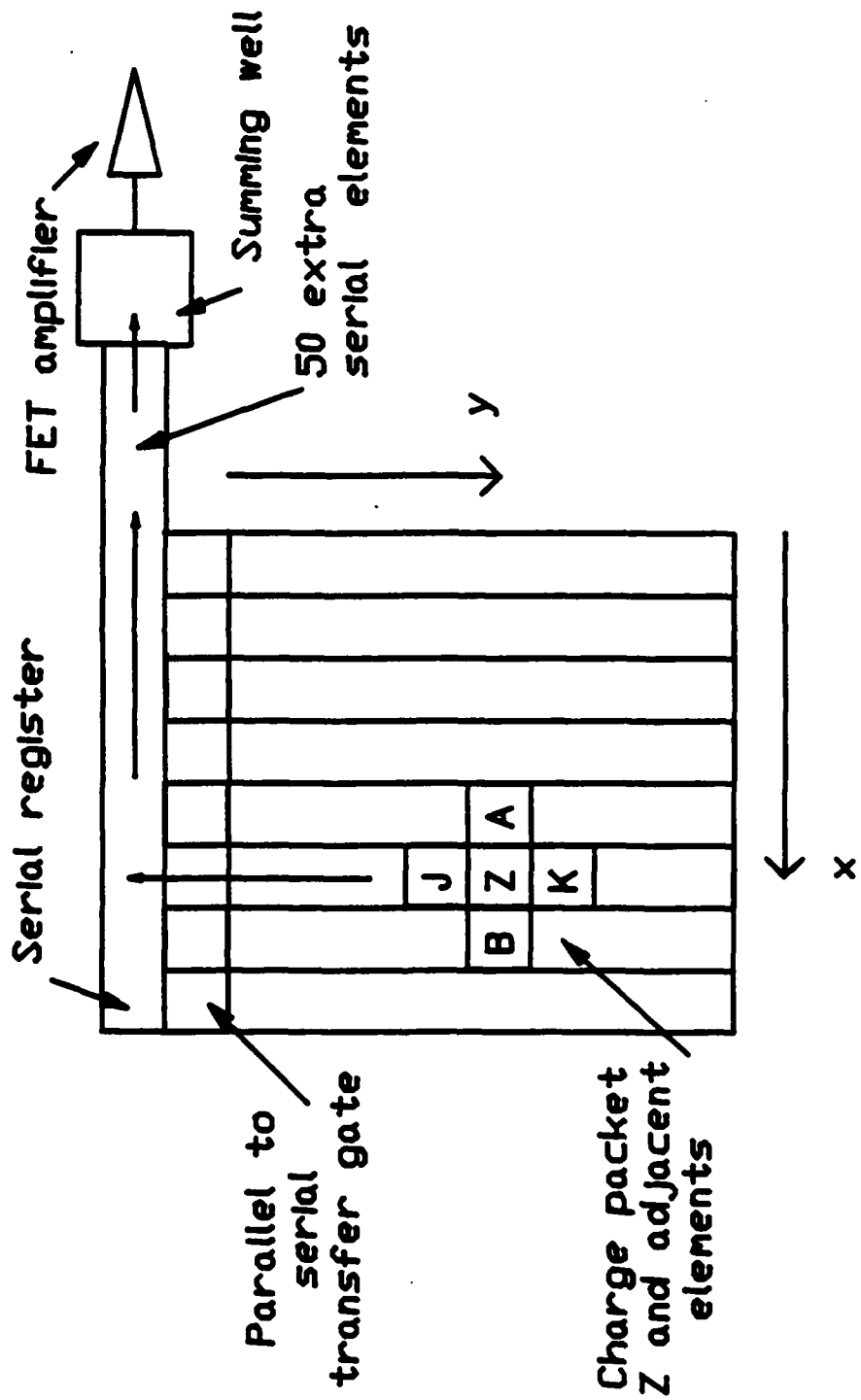


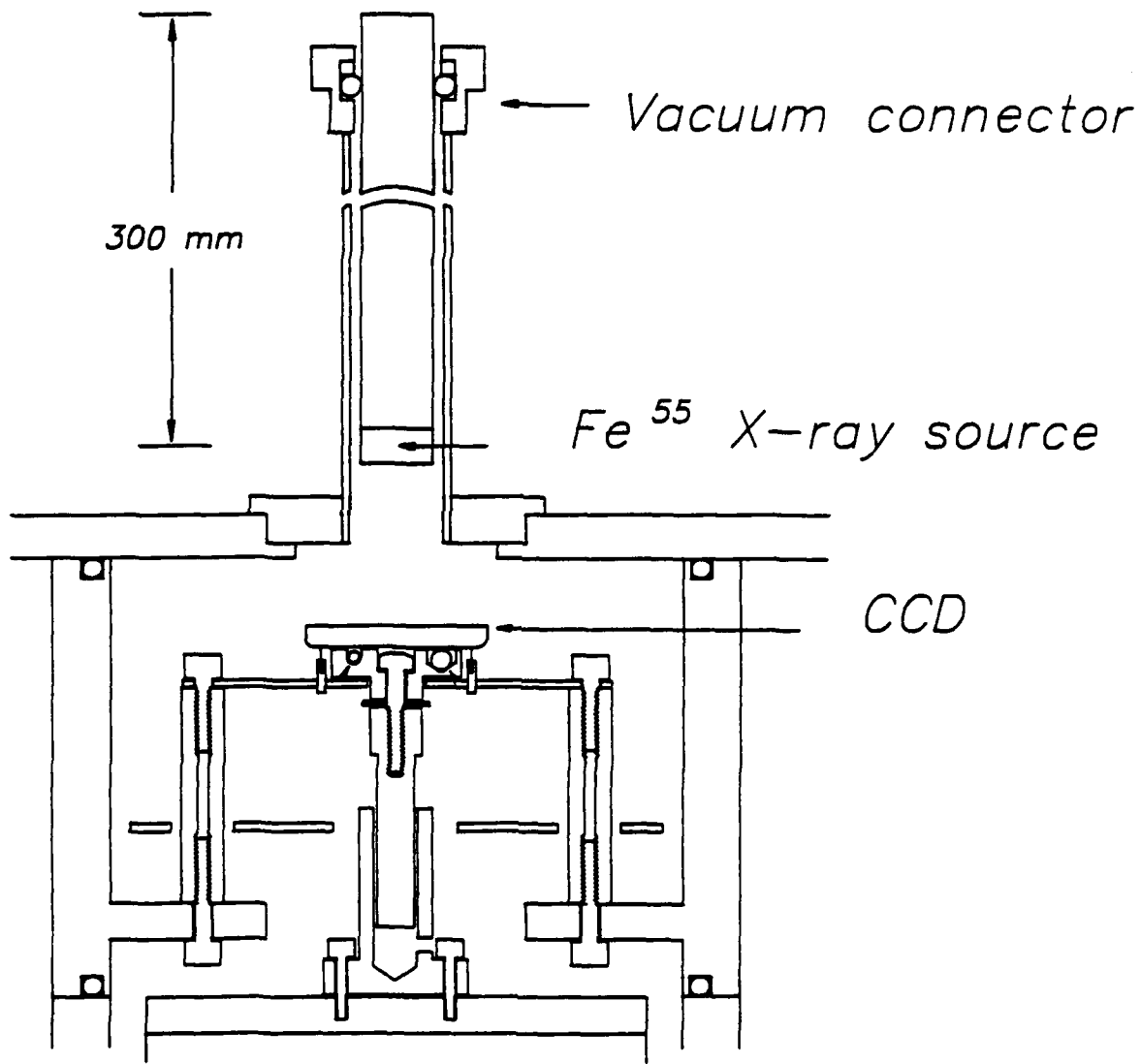


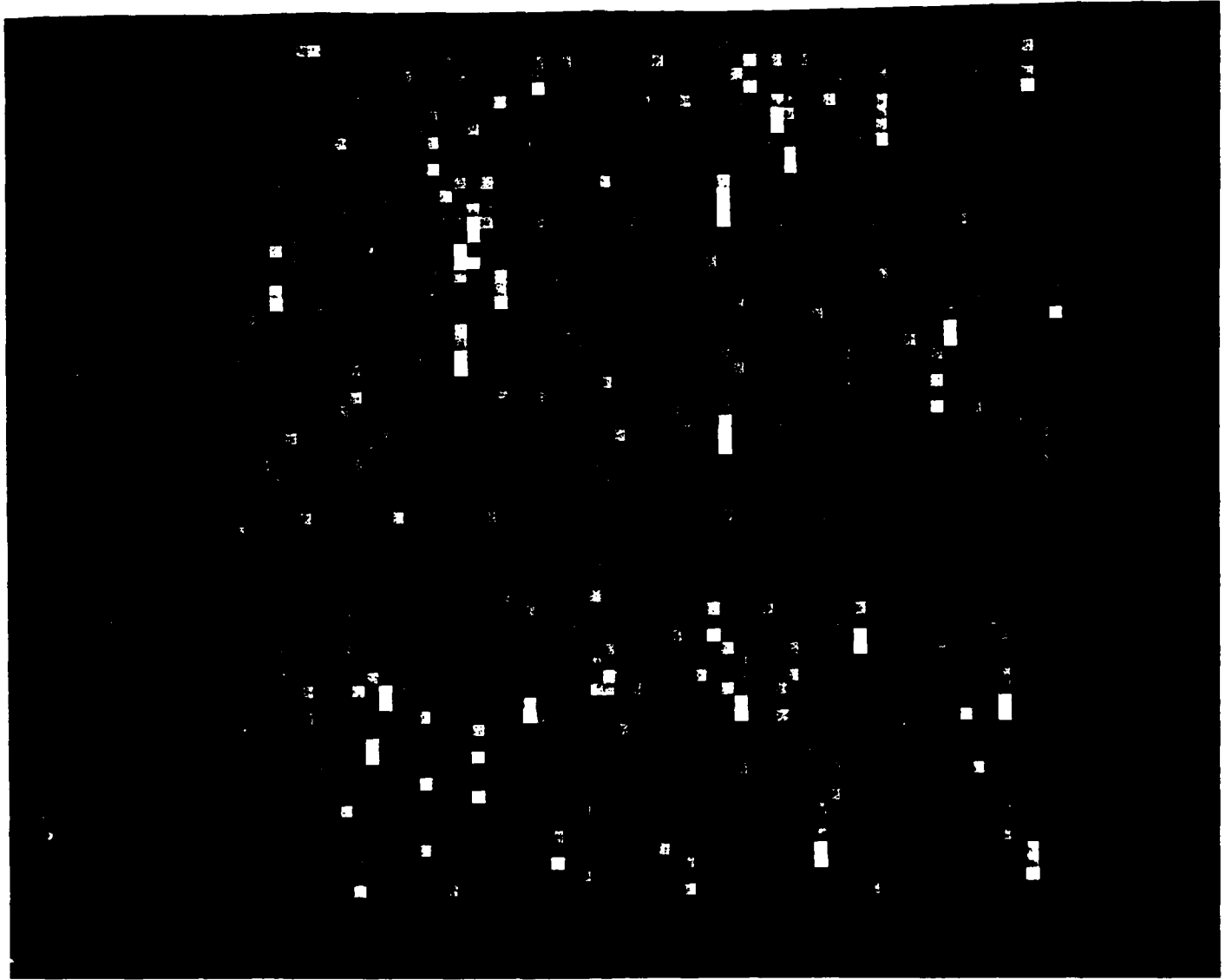


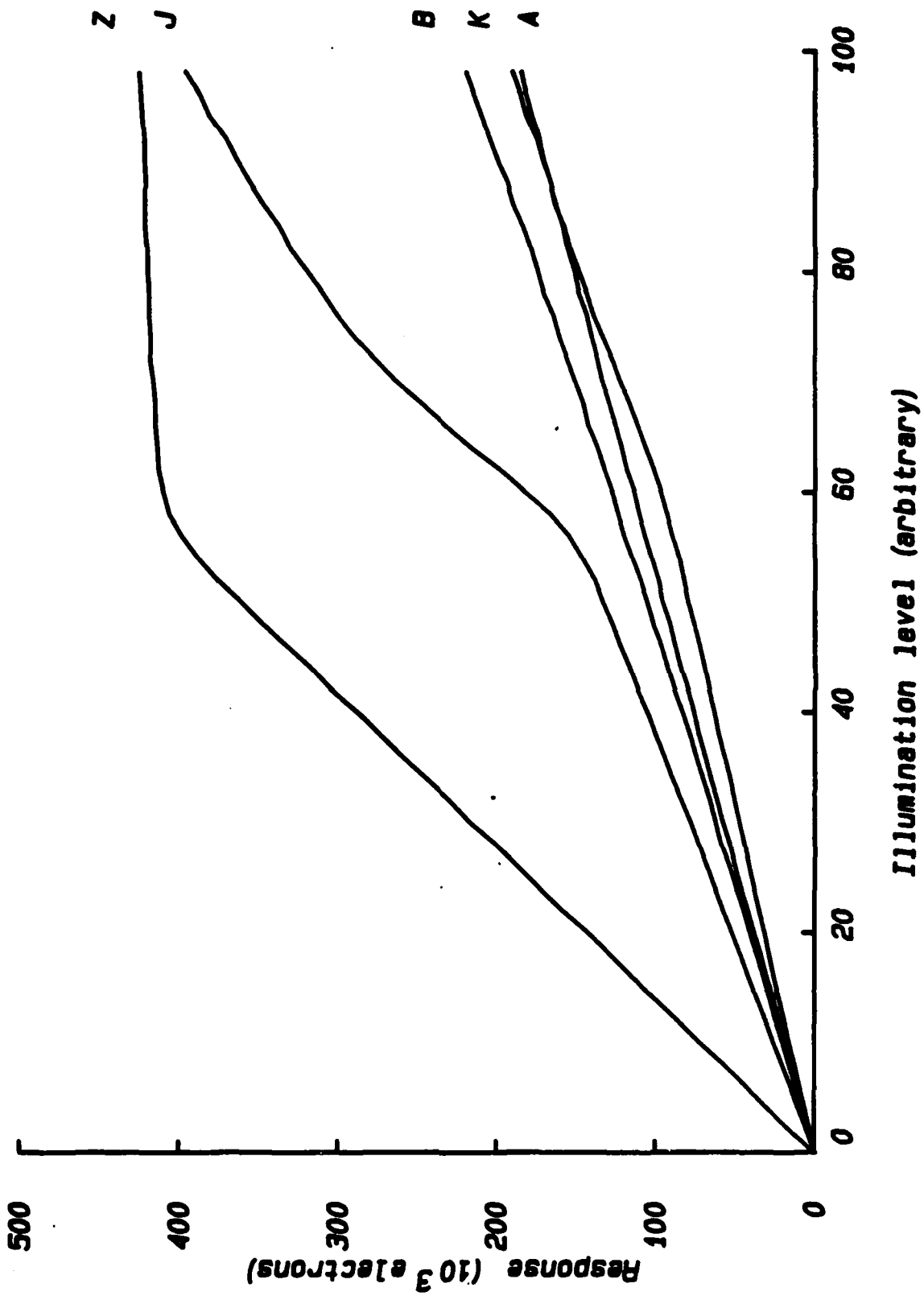












Captions for figures 1 to 9

Figure 1. Diagram of the signal processing chain used in the CCD detector system. Gain values are listed for each stage.

Fig. 2. Experimental setup used to measure noise of CCD output FET amplifier.

Figure 3. Mean value of a 32 by 32 subarray of the CCD for a uniformly increasing series of exposures. The largest deviations from a linear least squares line fit to the data are less than 100 e<sup>-</sup>. The relative maximum deviation from linearity as defined by the maximum deviation (100e<sup>-</sup>) divided by the highest illumination level ( $3 \times 10^5$  e<sup>-</sup>) is 0.03%.

Figure 4. Log of the dark count rate at several temperatures for the Tektronix frontside-illuminated CCD. At 142 K, 100 electrons are created in an one hour exposure, introducing ten electrons of noise into the image.

Figure 5. Quantum efficiency of the frontside illuminated CCD from 400 nm to 1000 nm. Peak quantum efficiency is 35% at 750 nm.

Figure 6. The readout path of a charge packet labeled Z, located at CCD coordinates x (serial direction) and y (parallel direction). Charge is transferred through y pixels in the image region and then transferred into the serial register by the parallel to serial transfer gate. Charge is then transferred through x + 50 elements of the serial register and then dumped into the summing well. Pixels adjacent to the central pixel in the serial shift direction are labeled A and B and in the parallel shift direction are labeled J and K.

Figure 7. Cross section diagram of Fe<sup>55</sup> x-ray source used to measure charge transfer efficiency. The slide rod arrangement allows the source to be positioned 1 to 250 mm from the CCD while under vacuum. By positioning the source at different distances, the x-ray flux is easily altered. The x-ray source takes the place of the window assembly and is easily attached to the CCD Dewar.

Figure 8. Image of 4 second exposure of CCD to x-ray source. Image is a 64 by 64 subarray of CCD located at the corner farthest from the output amplifier. Note the trailing of charge in the serial (horizontal) direction.

Figure 9. Typical blooming plot describing the response of a central element Z and 4 adjacent detector elements as a function of the illumination level of the central element (see Fig. 6 for notation of pixels). The slope of the response of pixel J increases at the same illumination level as the slope of Z goes to zero, indicating that charge has spilled during transfer in the parallel register from element Z into element J.

**Table 1**  
**CCD FET Amplifier Typical Analyzed Data Set**

Vd volts	Vg volts	Vs volts	Gfs mho	Gain	Rout ohms	En dbv	FOM	En nv/Hz	Electrons rms
22	1.2	6.17	220	0.81	3704	-120.0	118.22	18.26	10.34
20	1.2	6.15	220	0.81	3704	-122.0	120.22	14.50	8.21
18	1.2	6.12	220	0.81	3704	-123.0	121.22	12.93	7.32
16	1.2	6.11	210	0.81	3846	-124.0	122.14	11.52	6.52
14	1.2	6.09	200	0.80	4000	-125.5	123.56	9.96	5.49
12	1.2	6.07	180	0.78	4348	-127.0	124.87	8.16	4.62
10	1.2	6.04	180	0.78	4348	-126.5	124.37	8.64	4.89
8	1.2	6.00	160	0.76	4762	-126.5	124.14	8.64	4.89

**Table 2**  
**Parallel and Serial CTE of Tektronix 512M-001 CCD**

Temperature (K)	CTE <sub>s</sub>	CTE <sub>s-&gt;sw</sub>	CTE <sub>p</sub>	CTE <sub>p-&gt;s</sub>
183	.99989	.977	.999993	.995
161	.99987	.972	.999995	.995
130	.99986	.942	.999966	.975

**Table 3**  
**Onset of Blooming of Tektronix 512M-011 CCD in Electrons**

**Summing Well  $6.2 \times 10^6$  (electrons)**

**Serial Register**

<b>Upper Clock Level (volts)</b>	<b>Lower Clock Level (volts)</b>	<b>Blooming Onset (electrons)</b>
+9 volts	-4 volts	$.48 \times 10^6$
+12 volts	-8 volts	$.94 \times 10^6$

**Parallel Register**

<b>Upper Clock Level (volts)</b>	<b>Lower Clock Level (volts)</b>	<b>Blooming Onset (electrons)</b>
+4 volts	-6 volts	$.92 \times 10^6$
+8 volts	-6 volts	$1.1 \times 10^6$

**Table 4**

**Summary of Tektronix 512M-011 CCD Electro-Optical Performance  
(See text for operating conditions)**

<b>Output FET Noise</b>	<b>5 - 12 Electrons</b>
<b>Linearity</b>	<b>0.03% Maximum Deviation</b>
<b>Thermal Generation of Charge</b>	<b>0.03 Electrons/Sec @ 142K</b>
<b>Quantum Efficiency</b>	<b>35% @ 750 nm Maximum</b>
<b>CTE Parallel Register</b>	<b>0.999995 @ 161K</b>
<b>CTE Serial Register</b>	<b>0.99987 @ 161K</b>
<b>Blooming Onset Parallel Register</b>	<b>&gt; 900,000 Electrons</b>
<b>Capacity Output Summing Well</b>	<b>&gt; 6,000,000 Electrons</b>

END

9-87

Dtic